http://dx.doi.org/10.5012/bkcs.2013.34.6.1779

Optical Properties and Field Emission of ZnO Nanorods Grown on p-Type Porous Si

Taehee Park, Eunkyung Park,[a] Juwon Ahn,[b] Jungwoo Lee,[c] Jongtaek Lee, Sang-hwa Lee,[†] Jae-yong Kim,[†] and Whikun Yi[*]

Department of Chemistry and Research Institute for Natural Science, Hanyang University, Seoul 133-070, Korea
[*]E-mail: wkyi@hanyang.ac.kr
[†]Department of Physics, Hanyang University, Seoul 133-070, Korea
Received January 29, 2013, Accepted March 20, 2013

N-type ZnO nanorods were grown on p-type porous silicon using a chemical bath deposition (CBD) method (p-n diode). The structure and geometry of the device were examined by field-emission scanning electron microscopy (FE-SEM) and X-ray diffraction (XRD) while the optoelectronic properties were investigated by UV/Vis absorption spectrometry as well as photoluminescence and electroluminescence measurements. The field emission (FE) properties of the device were also measured and its turn-on field and current at 6 V/μm were determined. In principle, the growth of ZnO nanorods on porous siicon for optoelectronic applications is possible.

Key Words : n-Type ZnO nanorod, Porous silicon, Photoluminescence, Electroluminescence, Field emission

Introduction

ZnO has attracted much attention within the scientific community as a 'future material'.[1] The interest in this material has arisen due to the development of growth technologies for the fabrication of high quality single crystals and epitaxial layers, allowing for the realization of ZnO-based electronic and optoelectronic devices.[2,3] ZnO has a wide range of properties that depend on doping including a range of conductivities from metallic to insulating, high transparency, piezoelectricity, wide band gap semiconductivity, and chemical sensing effects. Many different groups have focused on novel nanostructures with different shapes ranging from nanowires to nanobelts and even nanosprings.

At ambient pressure and temperature, ZnO crystals possess a wurtzite structure. This is a hexagonal lattice and is characterized by two interconnecting sublattices of Zn^{2+} and O^{2-}, such that each Zn^{2+} ion is surrounded by a tetrahedra of O^{2-} ions and vice-versa. This tetrahedral coordination gives rise to polar symmetry along the hexagonal axis. This polarity is responsible for a number of the properties of ZnO, including its piezoelectricity and spontaneous polarization, and is also a key factor in its crystal growth, etching, and defect generation. Many groups have focused on novel nanostructures with different shapes ranging from nanowires to nanobelts and even nanosprings. ZnO nanorods or nanowires are generally synthesized by four main techniques: chemical vapor deposition,[4] metal-organic vapor deposition,[5] an aqueous solution method (equivalent to chemical bath deposition (CBD)),[6] and electrodeposition.[7] In spite of many previous studies of ZnO synthesis on various substrates[8,9] or porous templates,[10,11] ZnO nanorod films grown on porous silicon (PS) have been rarely studied. PS is one of the most important Si-based materials because its open structure and large surface area, combined with its unique optical and electrical properties, open up opportunities for its use as templates.[12,13]

Here, we report highly oriented ZnO nanorod films synthesized on PS templates using the CBD technique after deposition of a seed layer of ZnO. The optoelectronic and electronic properties of the devices were evaluated by measuring their photoluminescence (PL), electroluminescence (EL) spectra, and field emission (FE). Their structures and energy levels are also discussed in terms of the above mentioned results and X-ray diffraction (XRD) data.

Experimental

The PS substrate was made by an electrochemical anodization method[14-16] on p-type Si (100) substrate possessing a resistivity of 1-20 Ω·cm. Al (100 nm) was deposited on the back side of the substrate to form the electrode as the anode while a Pt plate served as the cathode (counter electrode). Electrochemical anodization was carried out for 20 min in a Teflon cell containing a HF:ethanol:de-ionized (DI) water solution (1:2:1 volume ratio) with a current density of 50 mA/cm^2. A 50 W halogen lamp was used for the back side illumination for the deviation of effective holes during the electrochemical anodization. The resultant PS had about a 20-30 μm thick porous layer. After the etching process, the substrate was rinsed using DI water and dried in a nitrogen atmosphere.

The synthesis of ZnO nanorods was conducted by applying the aqueous solution method.[17] First, we made a ZnO

[a]Present address: 533. Hogye-dong, Dongan-gu, Anyang-City, Gyeonggi-do 431-749, Korea
[b]Present address: 1B-92Lot, 816, Wonsi-dong, Danwon-gu, Ansan-City, Gyeonggi-do 425-852, Korea
[c]Present address: 104-1, Moonji-dong, Yuseong-gu, Daejeon, 305-738, Korea

seed layer to form a dense structure. The ZnO seed layer was prepared by RF sputtering, as it is able to produce large, well-oriented, and uniform ZnO films even on amorphous substrates at high deposition rates.[18,19] M. Katoda *et al*. reported that ZnO films fabricated in RF mode sputtering systems showed excellent piezoelectric properties and c-axis orientation. The sputtering system consisted of a cylindrical ZnO target. The deposition with Ar gas (13 sccm) at 150 W was conducted in a vacuum chamber. Second, plastic bottles were filled with a mixture of a 0.02 M equimolar aqueous solution of zinc nitrate hexahydrate ($Zn(NO_3)_2{\cdot}6H_2O$) and hexamethylenetetramine (HMT: $C_6H_{12}N_4$). Subsequently, PS substrates were placed in the bottles and heated at a constant temperature of 70 ºC for 24 h. Finally, the thin films grown on the substrates were washed with DI water to eliminate residual salts, dried in air, and annealed at 400 ºC. An annealing process was essential to remove the residual organic material and improve the crystallinity of the ZnO nanorods.

The crystalline character and structures were examined by XRD (D/MAX-2500/PC) and field-emission scanning electron microscopy (FE-SEM: JSM-6701F), respectively. The optoelectronic properties including the PL (PC-1) and EL were also measured. Finally, the FE properties of the synthesized ZnO nanorods on p-type PS were measured. FE current-voltage (I-V) curves were measured at room temperature in a vacuum chamber at a pressure of 1.0×10^{-6} Torr. The anode used to collect electrons was indium tin oxide (ITO) and general mesh was used as the cathode. A Teflon spacer with a thickness of 150 μm and an aperture area of 0.32 cm^2 was inserted between the anode and sample on the cathode. The FE currents were recorded using an ampere meter (Keithley 6517).

Results and Discussion

Figure 1(a) and (c) show the front and vertical FE-SEM images of p-type PS. The images clearly shows a rough surface etched by the electrochemical method. Figure 1(b) and (d) show FE-SEM images of ZnO nanorods grown on a p-type PS substrate. ZnO nanorods grown on p-type PS have a wurtzite structure and the tips of the ZnO nanorods appear to be a well-defined hexagonal plane. To investigate the growth mechanism of this novel ZnO nanostructure grown on p-type nanoporous silicon, FE-SEM images were obtained while adjusting the growth time and concentration of the ZnO precursor solution. During the hydrothermal fabrication, the ZnO seed-adsorbed sites can serve as good nucleation sites of the ZnO precursor at the elevated solution temperature, leading to the formation of a nanorod array of ZnO films on the surface of the nanoporous film. Due to the nanoporous surface of p-type PS, ZnO nanorods are grown at various angles. With the depletion of the precursor and the decreasing growth rate as the reaction time increases, other ions may also be adsorbed on the surface of the dense ZnO nanorod layer, which may result in the random growth of ZnO nanorods.

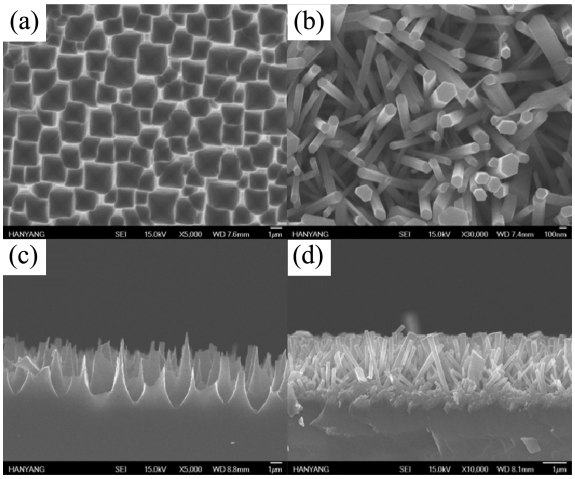

Figure 1. FE-SEM images of the (a) surface of p-type PS, (b) surface of ZnO nanorods on p-type PS, (c) cross-section of p-type PS, and (d) cross-section of ZnO nanorods on p-type PS.

Figure 2 shows the XRD results of the ZnO nanorod films formed on p-type PS. The structural and lattice parameters of the product were analyzed using XRD operated at 40 kV and 100 mA with Cu Kα radiation. All of the diffraction peaks could be assigned to hexagonal ZnO. It is well known that vertically-aligned ZnO nanorod arrays can be obtained on Si (111) or ZnO (111) substrates with a maximum intensity at $2\theta = 34.5^{o}$ ((002) Miller index).[20] Fragala *et al.* also reported vertically-grown ZnO nanorods on the Si (111) plane by texturing Si (100) substrates. Their XRD peaks showed the highest intensity at ZnO (002). However, the (100), (101), and (103) peaks in Figure 2 are higher than the other peaks. This result can be attributed to the roughness of the PS substrate. Previously, the XRD peaks of ZnO nanorods were measured on randomly-oriented ZnO nanorods on various substrates,[21] where the intensity of the (002) peak was lower than those of (100) and (101) peaks. Our XRD results are consistent with the random growth of the ZnO nanorods observed in the images in Figure 1.

Figure 3(a) shows the UV/Vis absorption spectrum of the ZnO nanorods on p-type PS. The maximum absorption peak

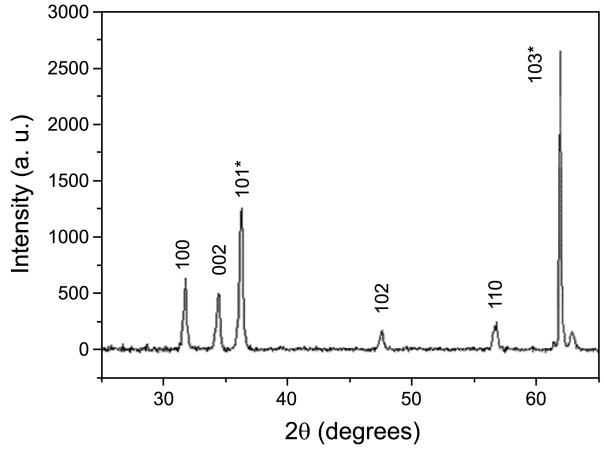

Figure 2. Indexed XRD pattern of ZnO nanorods grown on p-type PS.

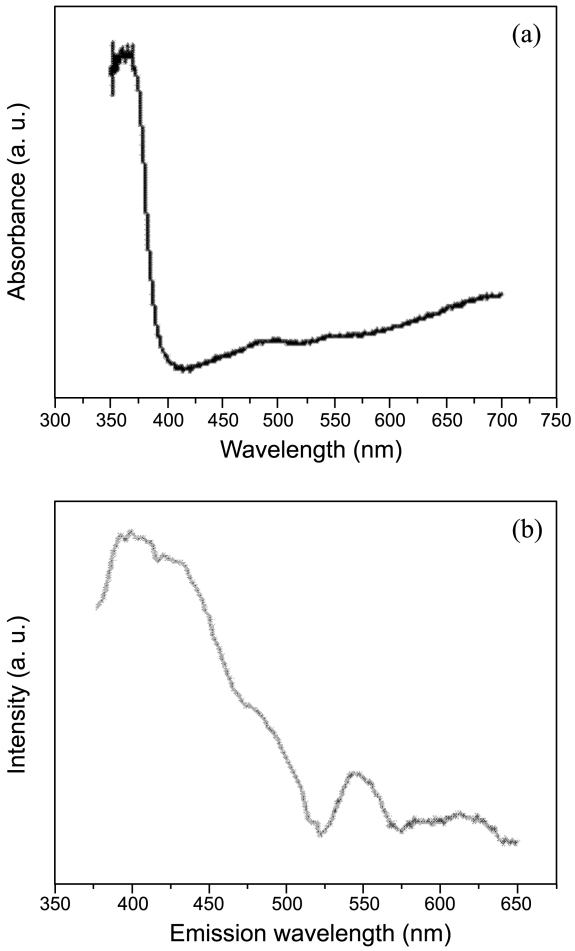

Figure 3. (a) UV absorption spectrum of ZnO nanorods grown on p-type PS and (b) room temperature PL spectrum of ZnO nanorod thin films on p-type PS.

of ZnO occurred at about 375 nm. The absorption of the UV spectrum is related to the bandgap of ZnO. Bandgaps can be estimated using the Urbach model[22] by fitting the absorption coefficient, α, to an equation. By applying this theory, the estimated bandgap energy of ZnO nanorods grown by using a dipping method in a ZnO nanoparticle solution on p-type PS is 3.30 eV. Figure 3(b) shows the room temperature PL spectrum of the sample. An excitation wavelength of 320 nm was applied to the ZnO nanorod layer. UV, blue, and green emissions were observed from the ZnO nanostructures on the PS substrate. Usually, the PL spectrum of ZnO is composed of ultraviolet emission from free excitons and a visible blue-green band related to deep-level defect emission.[23] The UV emission is also called the near band edge (NBE) emission and it originates due to the recombination of free excitons through the exciton-exciton collision process.[24] Dai *et al*. reported that blue emission at 460 nm may be due to intrinsic defects such as oxygen and zinc interstitials.[25] The green emission is also known to be a deep level emission (DPE), which is caused by the impurities and structural defects in the crystal such as oxygen vacancies and zinc interstitials.[26]

The EL measurements were performed based on ZnO nano-

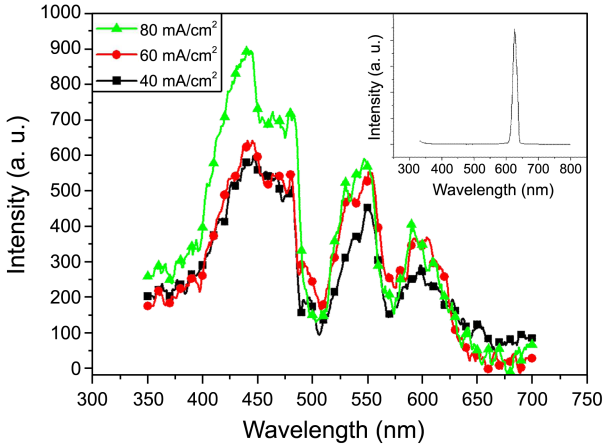

Figure 4. EL spectra of ZnO nanorods grown on p-type PS at different applied currents. The inset represents the PL peaks of p-type PS.

rods on p-type PS at room temperature. The EL emissions gradually became intense with increasing injection current. A broader blue excitonic emission at 450 nm and a defect related emission at 550 nm from ZnO nanorods[27] are observed in Figure 4. The 610 nm emission is related to p-type PS,[28] as shown in the inset of Figure 4. The origin of the EL is a result of the recombination of the electron-hole pair. This electron-hole pair is generated by the electron excited to the conduction band, where it can be trapped and recombine with the hole left in the valence band. This process gives rise to the emission centered at 450 nm.

Emission of electrons from a nanostructure when subjected to an external electric field is of great commercial interest in displays and other electronic devices. The emission properties of the nanostructures can be generally improved by controlling the geometry (aspect ratio) and spatial distribution (alignment and density) of nanomaterials.[29] electrons injected in the semiconductor layer. In addition, it is also possible to improve the emission of electrons by tailoring the workfunction of the materials.[30] Figure 5 shows the FE curve of our sample. The turn-on field of the ZnO nanorods

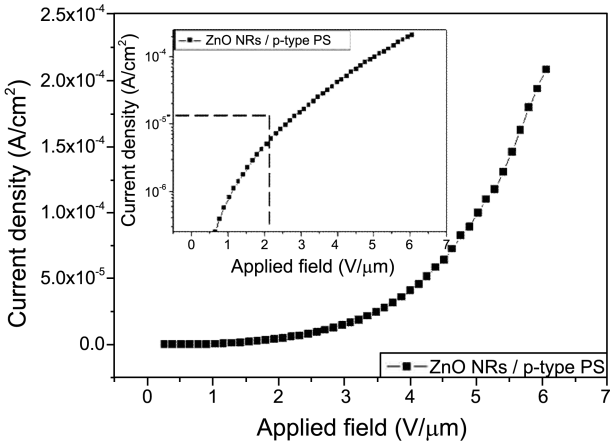

Figure 5. The FE current-voltage curve of ZnO grown on p-type PS. The inset shows the log scale of the current-voltage curved used to determine the turn-on field of the ZnO nanorods.

grown on p-type PS substrate, $V_{T\text{-}O}$, which is defined as the field to produce a current density of 10 μA/cm^2, was measured to be 2.7 V/μm and the emission density was 0.2 mA/cm^2 at an applied field of 6 V/μm. In addition to carbon nanotubes, ZnO nanomaterials are a widely studied class of field-emitting nanostructures because of their stability in oxidizing conditions.[31] It has been proven that the FE efficiency not only depends on the intrinsic properties of a nanostructure, but also on other factors such as the substrate, coating effect, and surface treatment. With these results, we believe that ZnO nanorods on porous structures can be used as electron emitters for nanodevices and displays.

Conclusion

Well-directed ZnO nanorods were fabricated on p-type PS substrates via CBD. The n-type ZnO nanorod films can form a good p-n heterojunction with a p-type PS substrate. We observed blue and green emissions from the ZnO nanorods and red emission from the p-type PS. The ZnO nanorods/p-type PS nanocomposite films can be used as a solid source of white light emission in various potential applications. It was found that the sharp geometry can substantially enhance the emission. In addition, our sample exhibited a high emission current density and a low turn-on voltage, which make it a potential candidate for further applications.

Acknowledgments. This study was supported by the National Research Foundation of Korea Funded by the Ministry of Education, Science, and Technology (KRF-2011-0028850 and 2011-0027329).

References

1. Bunn, C. W. *Proc. Phys. Soc. London* **1935**, *47*, 835.
2. Gudiksen, M. S.; Lauhon, L. J.; Smith, D. C.; Lieber, C. M. *Nature* **2002**, *415*, 617.
3. Haung, Y.; Daun, X. F.; Cui, Y.; Lauhon, L. J.; Kim, K. H.; Libber, C. M. *Science* **2001**, *294*, 1313.
4. Wagner, R. S.; Eliss, W. C. *Appl. Phys. Lett.* **1964**, *4*, 89.
5. Lee, W.; Jeong, M. C.; Myoung, J. M. *Nanotechnology* **2004**, *15*, 144.
6. Drici1, A.; Djeteli, G.; Tchangbedji, G.; Derouiche, H.; Jondo, K.; Napo, K.; Bernède, J. C.; Ouro-Djobo, S.; Gbagba, M. *Phys. Stat. Sol. (A)* **2004**, *201*, 1528.
7. Vergeìs, M. A.; Mifsud, A.; Serna, C. J. *J. Chem. Soc. Fara. Transac.* **1990**, *86*, 959.
8. Ko, H. J.; Chen, Y. F.; Zhu, Z.; Yao, T.; Kobayashi, I.; Uchiki, H. *Appl. Phys. Lett.* **2000**, *76*, 1905.
9. Ohtomo, A.; Tamura, K.; Saikusa, K.; Takahashi, T.; Makino, T.; Segawa, Y.; Koinuma, H.; Kawasaki, M. *Appl. Phys. Lett.* **1999**, *75*, 2635.
10. Zhang, W. H.; Shi, J. L.; Wang, L. Z.; Yan, D. S. *Chem. Mater.* **2000**, *12*, 1408.
11. Li, Y.; Meng, G. W.; Zhang, L. D.; Phillipp, F. F. *Appl. Phys. Lett.* **2000**, *76*, 2011.
12. Look, D. C. *J. Electron. Mater.* **2006**, *35*, 1299.
13. Ahsanulhaq, Q.; Umar, A.; Hahn, Y. B. *Nanotechnology* **2007**, *18*, 115603.
14. Xu, D.; Guo, G.; Gui, L.; Tang, Y.; Shi, Z.; Jin, Z.; Gu, Z.; Liu, W.; Li, X.; Zhang, G. *Appl. Phys. Lett.* **1999**, *75*, 481.
15. Sohn, J. I.; Lee, S.; Song, Y.-H.; Choi, S.-Y.; Cho, K.-I.; Nam, K.-S. *Appl. Phys. Lett.* **2001**, *78*, 901.
16. Li, J.; Lei, W.; Zhang, X.; Wang, B.; Ba, L. *Solid State Electron.* **2004**, *48*, 2147.
17. Ahsanulhaq, Q.; Umar, A.; Hahn, Y. B. *Nanotechnology* **2007**, *18*, 115603.
18. Ieki, H.; Tanaka, H.; Koike, J.; Nishikawa, T. *IEEE MTT-S Dig.* **1996**, 409.
19. Ondo-Ndong, R.; Pascal-Delannoy, F.; Boyer, A.; Giani A.; Foucaran, A. *Material Science and Engineering: B* **2003**, *97*, 68.
20. Fragalà, M. E.; Mauro, A. D.; Litrico, G.; Grassia, F.; Malandrino, G.; Foti, G. *Cryst. Eng. Comm.* **2009**, *11*, 2770.
21. Sriparna, C.; Smita, G.; Avesh, K. T.; Pushan, A. *J. Nanosci. Nanotechnol.* **2011**, *11*, 10379.
22. Caglar, M.; Ilican, S.; Caglar, Y. *Thin Solid Films.* **2009**, *517*, 5023.
23. Wu, X. L.; Siu, G. G.; Fu, C. L.; Ong, H. C. *Appl. Phys. Lett.* **2001**, *78*, 2285.
24. Umar, A.; Karunagaran, B.; Suh, E. K.; Hahn, Y. B. *Nanotechnology* **2006**, *17*, 4072.
25. Dai, L.; Chen, X. L.; Wang, W. J.; Zhou, T.; Hu, B. Q. *J. Phys.: Condens. Matter* **2003**, *15*, 2221.
26. Vanheusden, K.; Seager, C. H.; Warren, W. L.; Tallant D. R.; Voigt, J. A. *J. Appl. Phys.* **1996**, *79*, 7938.
27. Fang, X.; Li, J.; Zhao, D.; Shen, D.; Li, B.; Wang, X. *J. Phys. Chem. C* **2009**, *113*, 21208.
28. Dimova-Malinovska, D.; Nikolaeva, M. *Vacuum* **2003**, *69*, 227.
29. Li, L.; Fang, X. S.; Chew, H. G.; Zheng, F.; Liew, T. H.; Xu, X. J.; Zhang, Y. X.; Pan, S. S.; Li, G. H.; Zhang, L. D. *Adv. Funct. Mater.* **2008**, *18*, 1080.
30. Pan, H.; Zhu, Y.; Sun, H.; Feng, Y.; Sow, C. H.; Lin, J. *Nanotechnology* **2006**, *17*, 5096.
31. Hong, W. K.; Sohn, J. I.; Song, S.; Lee, T. *Nano Lett.* **2008**, *8*, 950.